Supplemental material

Validation of the aerosol transport model

Remote-sensing and in situ aerosol observations are not available over many Arctic Ocean areas due to harsh sampling conditions, extensive cloud cover, high sea ice albedo, and the long periods of darkness during polar night. To understand as best we can how aerosol microphysics impacts clouds over the Arctic, we used the FLEXPART dispersion model with black carbon as a proxy for combustion aerosols to identify clean conditions in Arctic air masses, so that cloud properties in these conditions could be compared to general observations.

From the limited BC data that are available, the FLEXPART model appears to capture BC aerosol patterns very well over the Arctic[1–3]. Unfortunately, a lack of observations makes it difficult to validate model BC concentrations and spatial distributions over large swaths of the Arctic, particularly in the free troposphere and during polar night. Because spatial biases in the FLEXPART output could influence the meaningfulness of statistical comparisons between different locations, we validated FLEXPART BC output with Cloud-Aerosol Lidar and Infrared Pathfinder Satellite Observation (CALIPSO) aerosol layer data, which are the only nighttime aerosol data available regionally over the Arctic.

Vertical aerosol layer distribution was obtained from CALIPSO v. 4.10 level 2, 5-km merged aerosol and cloud layer data[4] at 532 nm. These data are collected at 30-m vertical

resolution up to 8.2 km, and at 75-m resolution between 8.2-8.5 km. Aerosol-containing profiles were required to be cloud-free and to have cloud-aerosol detection (CAD) scores > 70, indicating high confidence in cloud and aerosol separation.

CALIPSO aerosol profiles were used here for aerosol transport model validation. FLEXPART-derived clean conditions were more frequent at higher altitudes (Fig. 3), in line with previous observations of CALIPSO aerosol distributions[5]. Major uncertainties arise in this comparison because of the coarse vertical resolution of the FLEXPART model output, and because CALIPSO aerosols are not necessarily equivalent to BC concentrations. As such, it is unclear how thick an observed CALIPSO aerosol layer (measured in meters) must be to influence the average BC concentration in an altitude range equivalent to the FLEXPART model's vertical resolution (measured in kilometers). For these reasons, and because we use the aerosol model in this study only to identify clean (BC < 30 ng m-3) air masses, our validation efforts are focused mainly on assessing the likely locations of false negatives (i.e., where observations indicate that aerosol layers have a large impact on model-identified "clean" air masses), although information on false positives is provided as well.

To estimate model BC false negatives from CALIPSO aerosol distributions, we make several assumptions. First, we assume that combustion aerosols are the dominant aerosol source over the Arctic during polar night at the altitudes of relevance during this study (0.6-8.5 km). Ground-based data and aerosol transport models indicate that this is a fairly reasonable assumption[6,7]. Marine aerosols are mainly located in the shallow Arctic

47 boundary layer, whereas mineral dust can be found throughout the Arctic atmosphere but
48 in the free troposphere is often more homogeneously distributed than combustion
49 aerosols[8]. We also assume that the BC contribution to combustion aerosol mass is steady,
50 even though other studies have shown that BC:OC ratios, for example, can vary[9]. In cases
51 where the OC:BC ratio is higher than on average, FLEXPART would indicate relatively
52 too little aerosol compared to cases with a low OC:BC ratio. Other uncertainties are
53 introduced because CALIPSO cannot always identify dilute aerosol plumes[10], and it
54 sometimes misclassifies ice clouds with very small ice particles as aerosol layers[11].
55 Despite these uncertainties, information from this analysis is still very useful because of
56 how poorly the models are validated over large parts of the Arctic, particularly because
57 these models provide the only regional estimates of combustion aerosol concentrations
58 over large swaths of the Arctic.
59
60 Based on the above assumptions, model false negative rates in clean conditions are likely
61 to be highest when CALIPSO aerosol layers are observed in a large fraction of the model
62 altitude layer. Average "clean" FLEXPART vertical layers often contain some
63 CALIPSO-observed aerosol layers within them. These contribute on average to ~19-27%
64 of the layer volume (Fig. S3a). The actual BC concentrations of these aerosol layers are
65 unclear. Previous analysis indicates that CALIPSO misses ~33-36% of very dilute (30-50
66 ng BC m-3) combustion aerosol layers[1], and so the fractions estimated in Figure S3a
67 might actually underestimate aerosol layer presence somewhat.
68

However, CALIPSO aerosol volume contributions in clean conditions were significantly less at each altitude level than those found in all or polluted (BC >150 ng m-3) conditions (Wilcoxon rank test, $p<0.05$) (Fig. S4). Most altitudes also had no major clustering of high values in Figure S3a, which provides some confidence that model-identified clean conditions are at least comparable between large regions (e.g., over sea ice and over open ocean). The largest clustering in Figure S3a occurs at the lowest altitude level (0.6-1.5 km), where there was a slightly higher likelihood of false negatives over open ocean compared to sea ice. The highest overall likelihood of false negatives occurred at the highest altitude level (6-8.5 km), but it was not much larger than at other altitudes (Fig. S4).

Previous analysis indicates that in nighttime clear-sky conditions, CALIPSO should detect non-dilute aerosol layers in profiles where FLEXPART reports median column BC concentrations greater than 150 ng m^{-3} [1]. Model false positive rates are likely to be highest when CALIPSO aerosol layers do not fill a large fraction of the model altitude layer where modeled BC was >150 ng m^{-3} (Fig. S3b). CALIPSO detected aerosol layers nearly all the time during clear nighttime conditions in some portion of the altitude bin where high BC concentrations were predicted. These aerosol layers contributed to 0.3-2.0 times more volume on average, depending on altitude, than in clean conditions. The likelihood of false positives was highest over the open ocean in the lower two altitude bins (0.6-2.5 km), which might have a small impact on our comparisons between sea ice and open ocean at these altitudes. Note that observed aerosol layers may be present in the

model, but could be displaced in altitude (e.g., by a kilometer or two), which could contribute to the apparent false positives or false negatives.

In summary, in model-estimated clean conditions, CALIPSO aerosol layers contributed significantly smaller volume than in all and model-identified polluted conditions. There were also no major spatial biases in the false negative rates that would preclude the regional comparisons between sea ice and open ocean regions. These observations, in combination with previously conducted model validation studies indicating that the model does represent aerosol transport over the Arctic well, provide confidence in the model's ability to identify clean conditions.

References

1. Zamora, L. M. *et al.* Aerosol indirect effects on the nighttime Arctic Ocean surface from thin, predominantly liquid clouds. *Atmos Chem Phys* **17,** 7311–7332 (2017).
2. Eckhardt, S. *et al.* Current model capabilities for simulating black carbon and sulfate concentrations in the Arctic atmosphere: a multi-model evaluation using a comprehensive measurement data set. *Atmos Chem Phys* **15,** 9413–9433 (2015).
3. Stohl, A. *et al.* Evaluating the climate and air quality impacts of short-lived pollutants. *Atmos Chem Phys* **15,** 10529–10566 (2015).
4. CALIPSO Science Team. CALIPSO/CALIOP Level 2, Lidar 5km Merged Aerosol and Cloud Layer Data, version 4.10, Hampton, VA, USA: NASA Atmospheric Science Data Center (ASDC), Accessed Nov. 2, 2017 at doi: 10.5067/CALIOP/CALIPSO/LID_L2_05kmMLay-Standard-V4-10. (2016).
5. Di Pierro, M., Jaeglé, L., Eloranta, E. W. & Sharma, S. Spatial and seasonal distribution of Arctic aerosols observed by the CALIOP satellite instrument (2006–2012). *Atmos Chem Phys* **13,** 7075–7095 (2013).
6. Quinn, P. K. *et al.* A 3-year record of simultaneously measured aerosol chemical and optical properties at Barrow, Alaska. *J. Geophys. Res.* **107,** 4130 (2002).
7. Stohl, A., Eckhardt, S., Forster, C., James, P. & Spichtinger, N. On the pathways and timescales of intercontinental air pollution transport. *J. Geophys. Res. Atmospheres* **107,** 4684 (2002).
8. Groot Zwaaftink, C. D., Grythe, H., Skov, H. & Stohl, A. Substantial contribution of northern high-latitude sources to mineral dust in the Arctic. *J. Geophys. Res. Atmospheres* **121,** 13,678-13,697 (2016).

9. Samset, B. H. *et al.* Aerosol Absorption: Progress Towards Global and Regional Constraints. *Curr. Clim. Change Rep.* 1–19 (2018). doi:10.1007/s40641-018-0091-4
10. Kacenelenbogen, M. *et al.* An evaluation of CALIOP/CALIPSO's aerosol-above-cloud detection and retrieval capability over North America. *J. Geophys. Res. Atmospheres* **119,** 230–244 (2014).
11. Di Pierro, M. Spatial and temporal distribution of Arctic aerosols: new insights from the CALIPSO satellite. (University of Washington, 2013).

Supplementary Figures

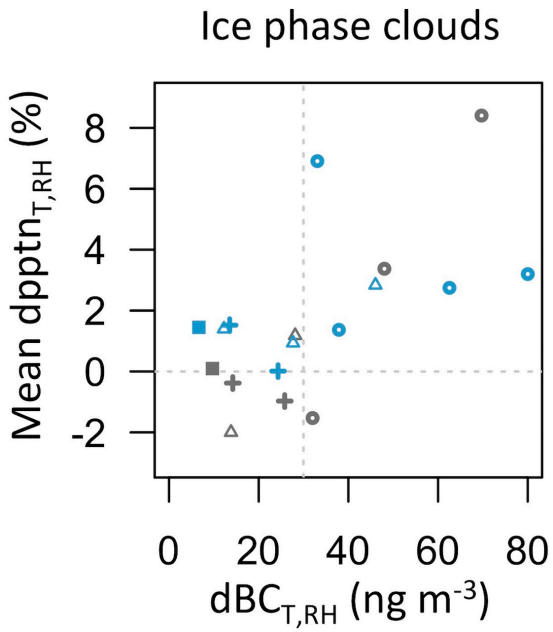

Figure S1. Mean IPC dpptn$_{T,RH}$ as a function of median dBC$_{T,RH}$ values within 10 ng m^{-3} BC increments. Values are shown for data over sea ice (grey) and open ocean (blue) at different altitudes between 0.6 and 6 km (open circles = 0.6-1.5 km, open triangles =1.5-2.5 km, crosses = 2.5-4 km, and filled squares = 4-6 km). In order to reduce the effects of outliers, each plotted data point represents at least 10 separate T/RH bins present in that altitude range, which in turn contain observations from at least 1250 km^2 over the Arctic Ocean. Thin light grey dashed lines indicate zero dpptn$_{T,RH}$ and a dBC$_{T,RH}$ value of 30 ng m^{-3}.

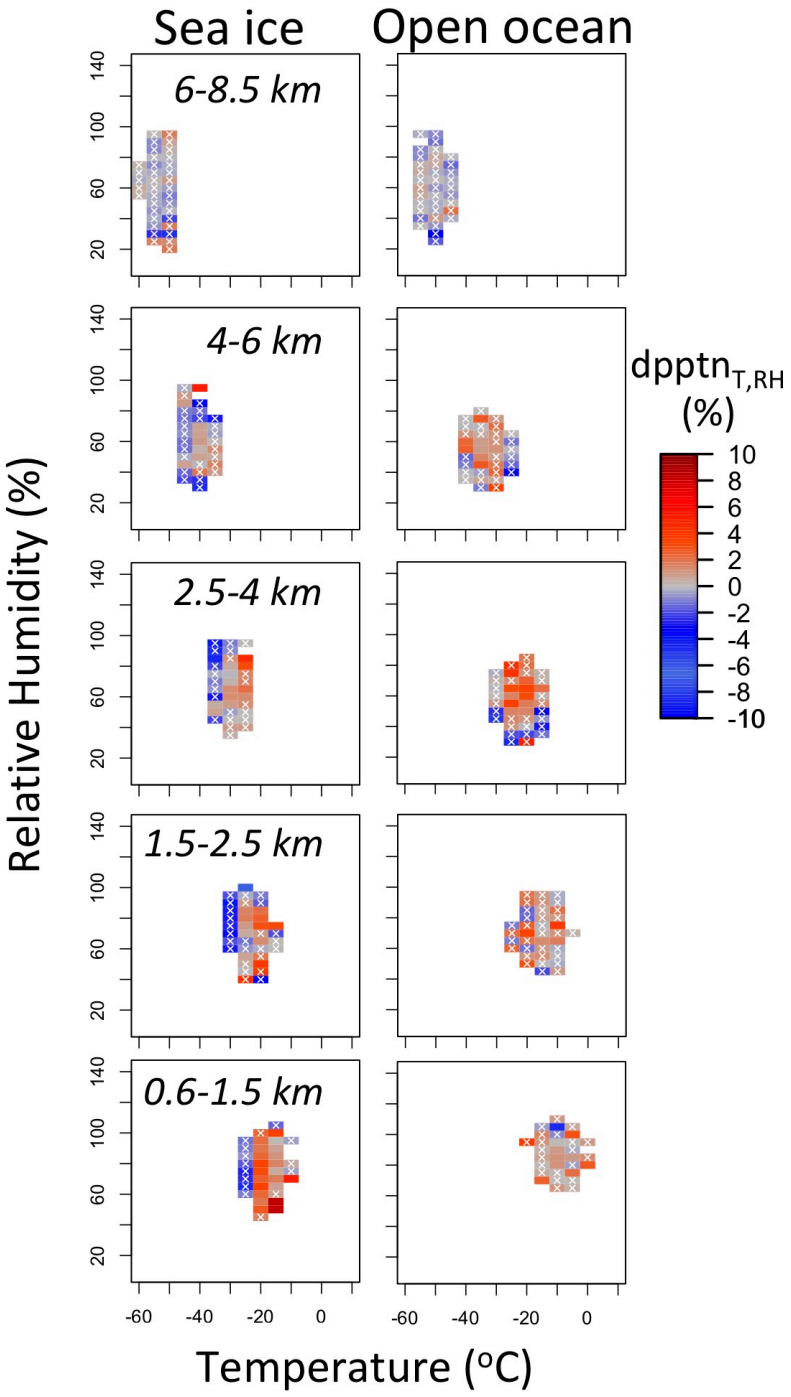

Figure S2. Same as for Figure 1, except for precipitation instead of cloud fraction. Here, individually significant cells numbered more than expected at random (binomial test, $p < 0.001$) at all levels except over open ocean between 1.5-2.5 km (significant at $p < 0.05$), and at 6-8.5 km (not significant).

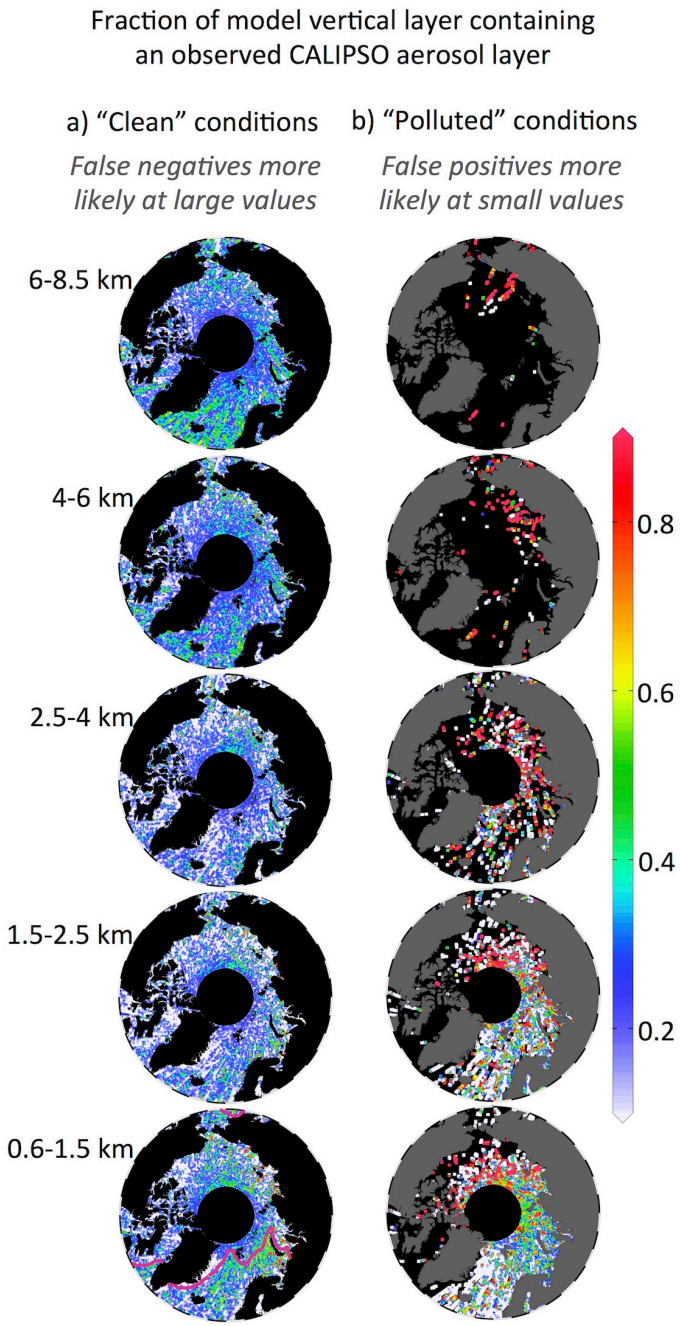

Figure S3. The fraction of different altitude layers in which CALIPSO aerosols were observed over the clear-sky nighttime Arctic Ocean, presented on a weighted average grid, when the FLEXPART model predicts a) clean conditions (BC < 30 ng m^{-3}), and b) polluted conditions (BC > 150 ng m^{-3}). We estimate that model false negatives and positives are most likely to occur where values in (a) are large and values in (b) are small, respectively, based on the assumptions that combustion aerosols are associated with BC and that they are the dominant aerosol source at these altitudes during polar night. The dark pink line on the bottom left represents sea ice extent during winter 2008-2009.

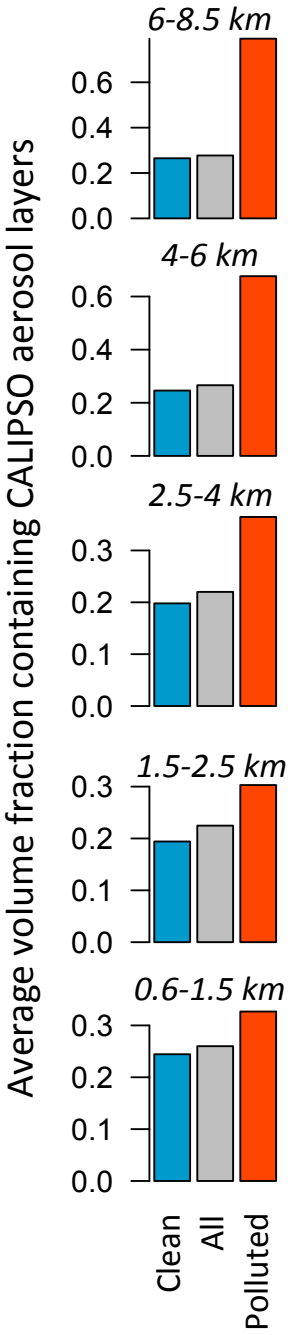

Figure S4. The average fraction of each altitude range containing observed CALIPSO aerosol layers for FLEPXART-determined clean (BC < 30 ng m^{-3}, blue), all (grey), and polluted (BC > 150 ng m^{-3}, red) conditions from ~500,000 clear air nighttime profiles between 2008-2009. Clean conditions had significantly smaller volumes occupied by aerosol layers than all or polluted conditions at every altitude, based on a Wilcoxon rank test, $p < 0.05$. Note different x-axes ranges in the plots.

Supplementary Tables

Table S1. The mean temperature (T, ^{o}C), relative humidity (RH, %), black carbon (BC, ng m^{-3}), and cloud fraction (CF, %) observed over the Arctic Ocean study region over sea ice and open ocean during different seasons and altitude levels. Data are shown for all conditions. Also shown are the mean differences between all minus clean conditions ("difference") for T, RH, BC, and CF, referred to as $\overline{dT}$, $\overline{dRH}$, $\overline{dBC}$, and $\overline{dCF}$ in the text.

		Sea ice						Open ocean					
	Altitude	Fall (ASO)		Winter (NDJ)		Spring (FMA)		Fall (ASO)		Winter (NDJ)		Spring (FMA)	
	levels (km)	all	difference	all	difference	all	difference	all	difference	all	difference	all	difference
Temperature (^{o}C)	6-8.5	-48.7	0.0	-53.0	0.0	-51.9	0.1	-45.0	0.1	-49.6	0.0	-49.2	0.1
	4-6	-32.3	0.5	-38.1	0.2	-40.0	0.4	-27.7	0.3	-33.2	0.1	-35.5	0.1
	2.5-4	-21.6	0.5	-27.5	0.1	-29.5	0.1	-15.8	0.4	-21.1	0.2	-23.6	0.0
	1.5-2.5	-15.5	0.5	-21.6	-0.4	-23.4	-0.7	-9.2	0.4	-14.6	0.4	-16.6	-0.2
	0.6-1.5	-11.3	0.4	-17.7	-0.6	-19.6	-1.3	-4.5	0.3	-9.9	0.4	-11.6	-0.3
Relative Humidity (%)	6-8.5	74.6	0.0	65.6	0.4	50.4	1.0	69.0	0.1	63.8	0.2	50.9	0.4
	4-6	61.5	-0.3	62.7	0.4	59.8	-0.6	57.1	-0.1	57.6	0.6	58.5	0.9
	2.5-4	66.7	-0.6	69.3	0.2	66.2	-1.8	61.4	0.2	58.6	1.6	57.1	0.6
	1.5-2.5	76.9	-0.9	74.0	-0.4	68.2	-0.3	74.5	0.2	72.5	1.9	69.1	0.5
	0.6-1.5	85.1	-0.3	78.1	-2.2	70.6	0.2	87.2	-0.3	88.6	1.7	84.4	-0.2
BC (ng m^{-3})	6-8.5	14	1	13	2	19	5	14	2	11	1	17	3
	4-6	17	3	22	6	30	11	17	3	18	3	28	9
	2.5-4	19.8	4	31	13	41	19	19	5	28	10	38	16
	1.5-2.5	20	4	39	21	53	27	22	7	43	23	47	22
	0.6-1.5	17	3	51	31	66	32	22	9	58	34	56	27
Mean CF (%)	6-8.5	15.4	0.2	15.0	0.4	9.1	0.9	19.3	1.0	22.3	0.4	15.3	0.5
	4-6	22.7	0.6	21.8	1.3	16.8	0.1	24.3	0.8	26.0	0.8	22.7	0.7
	2.5-4	29.1	1.0	25.9	1.0	20.8	-2.1	27.9	1.0	28.8	2.2	27.4	0.5
	1.5-2.5	35.0	-0.3	30.3	-0.4	24.0	-3.5	34.3	1.4	39.4	2.1	39.5	0.3
	0.6-1.5	33.3	-0.2	26.9	-2.0	22.0	-3.0	35.0	-0.3	43.0	-0.4	43.6	-0.3

Table S2. The data shown in Figure 3, indicating $dCF_{T,RH}$ (%), $dpptn_{T,RH}$ (%), $dCP_{T,RH}$ (%) and $dBC_{T,RH}$ (ng m^{-3}) values in different altitude ranges over sea ice and open ocean, weighted by number of cloud observations in each T/RH bin ($\overline{dCF_{T,RH}}$, $\overline{dpptn_{T,RH}}$, $\overline{dCP_{T,RH}}$, and $\overline{dBC_{T,RH}}$, respectively). Data are presented at different altitude ranges, and separately for IPCs, MPCs, and LPCs. Values of $\overline{dCF_{T,RH}}$ and $\overline{dpptn_{T,RH}}$ are expressed as the absolute change within the air volume of interest, with the bootstrapped 95% confidence intervals for the weighted mean in brackets. The values in square brackets are the relative percent change with respect to the value found in clean conditions. An asterisk (*) indicates significant differences between all and clean conditions based on a paired Wilcoxon rank test, $p < 0.05$, using T and RH grid cells containing > 800 (400) 12.5-km^2 gridded observations for $\overline{dBC_{T,RH}}$, $\overline{dCF_{T,RH}}$, and $\overline{dpptn_{T,RH}}$ ($\overline{dCP_{T,RH}}$). Values in bold indicate a significant change in $dCF_{T,RH}$, $dpptn_{T,RH}$ or $dCP_{T,RH}$ where $dBC_{T,RH}$ > 20 ng m^{-3} (Wilcoxon rank test, $p < 0.05$). The "Total (%)" values are the CP distributions in all conditions.

		Full dataset			Ice clouds			Mixed phase clouds			Liquid clouds		
	Altitude range (km)	$\overline{dBC_{T,RH}}$ (ng m^{-3})	$\overline{dCF_{T,RH}}$ (%)	$\overline{dpptn_{T,RH}}$ (%)	Total (%)	$\overline{dCP_{T,RH}}$ (%)	$\overline{dpptn_{T,RH}}$ (%)	Total (%)	$\overline{dCP_{T,RH}}$ (%)	$\overline{dpptn_{T,RH}}$ (%)	Total (%)	$\overline{dCP_{T,RH}}$ (%)	$\overline{dpptn_{T,RH}}$ (%)
Sea ice	6-8.5	**3**	0.4 (0.4-0.6) [3.5]*	-0.3 (-0.4-0.1) [-2.2]*	99	--	-0.4 (-0.5 to -0.2)*	1	--	0.3 (-0.1-1.4)	0	--	--
	4-6	**7**	**0.7 (0.6-0.9) [3.5]***	-0.3 (-0.4-0.1) [-1.2]	92	--	0.2 (0.1-0.5)	8	--	-0.1 (-0.3-0.4)	0	--	--
	2.5-4	**14**	**0.2 (0.1-0.5) [0.7]**	**0.1 (-0.1-0.6) [0.3]**	76	1.7 (1.5-1.1)*	0.5 (0.3-0.9)	23	-1.7 (-1.9 to -1.1)*	1.0 (0.8-1.7)	1	0.0 (0.0-0.2)	--
	1.5-2.5	**21**	**-1.1 (-1.2 to -0.7) [3.5]***	**0.0 (-0.1-0.5) [0.1]**	61	**4.7 (4.4-5.4)***	0.3 (0.1-0.9)	36	**-4.2 (-4.5 to -3.5)***	1.3 (1.1-2.0)*	3	**-0.4 (-0.5 to -0.1)***	--
	0.6-1.5	**27**	**-1.7 (-1.8 to -1.4) [-5.9]***	**0.9 (0.8-1.4) [3.0]***	49	6.5 (6.3-7.3)*	-0.6 (-0.8 to 0.2)	35	-2.9 (-3.1 to -2.2)*	1.5 (1.3-2.1)*	16	-3.7 (-3.8 to -3.1)*	0.0 (0.0-0.0)
Open ocean	6-8.5	**2**	0.8 (0.7-1.1) [4.0]*	-0.1 (-0.2 to 0.3) [-0.7]	93	--	-0.1 (-0.1-0.1)	7	--	-0.8 (-1.1 to -0.2)*	0	--	--
	4-6	**4**	0.5 (0.5-0.8) [2.3]*	0.7 (0.6-1.3) [3.1]*	78	--	0.9 (0.8-1.2)	20	--	0.3 (0.1-0.9)*	1	--	--
	2.5-4	**9**	1.1 (1.0-1.5) [4.2]*	**0.4 (0.2-1.1) [1.2]***	58	-1.0 (-1.2 to -0.3)*	1.5 (1.3-2.1)*	37	1.3 (1.1-2.0)*	0.9 (0.7-1.6)	6	-0.3 (-0.3 to 0.0)	-1.5 (-1.8 to -0.8)*
	1.5-2.5	**15**	**1.4 (1.3-1.7) [3.8]***	0.9 (0.7-1.3) [2.2]*	39	**-0.6 (-0.8-0.1)**	1.1 (0.9-1.6)*	47	**0.7 (0.5-1.4)**	0.1 (-0.1-0.7)	15	-0.2 (-0.3-0.3)	-0.1 (-0.3-0.2)
	0.6-1.5	**20**	-0.2 (-0.3-0.1) [-0.6]*	0.9 (0.8-1.3) [2.8]*	30	0.6 (0.4-1.1)	0.6 (0.4-1.2)	39	**0.5 (0.4-1.1)***	1.0 (0.7-1.6)*	31	-1.1 (-1.3 to -0.5)*	0.1 (0.1-0.2)